Canadian Mineralogist,
Vol. 11, pp. 791-811 (1972)

ELECTRONIC SPECTRA OF TRANSITION METAL IONS IN SILICATE GARNETS

RAYMOND K. MOORE * AND WILLIAM B. WHITE **

ABSTRACT

Electronic absorption spectra have been measured for 19 silicate garnets of widely varying composition. Measured changes in band intensity as a function of composition, and use of computer-generated energy level diagrams to fit the spectra have permitted some confirmation and modifications in the assignments of these very complex spectra.

INTRODUCTION

The absorption spectra of the silicate garnets in the visible and near ultraviolet regions are perhaps the most complicated observed for any mineral. As many as 15 to 20 distinct bands occur in the relatively narrow spectral range. These arise because of the variety of sites and the variety of transition metal ions that can substitute into the garnet structure. Much progress in understanding the garnet spectra has been reported in a series of papers by Manning (1967a, 1967b, 1969, 1970a, 1970b). Earlier work on the spectra of garnets has been reviewed by Manning and is not repeated here.

Because of the complexity of the spectra, some assignments and interpretations remain uncertain. In the present work, spectra of garnets have been measured over a wide composition range. Assignments can then be confirmed by following the change in band intensity with concentration of the responsible ion. Likewise the observed spectra were fitted to computer-generated energy level diagrams specific to the garnet sites, thus ensuring that all assignments were internally consistent. These procedures have confirmed some previous assignments and interpretations and have suggested modifications in others.

EXPERIMENTAL

A total of 19 garnet samples including ten pyralspites and nine ugrandites were used in this study. The samples were selected for crystallinity,

* Assistant Professor, Dept. of Natural Sciences, Radford College, Radford, Va.
** Professor, Materials Research Laboratory and Dept. of Geosciences, The Pennsylvania State University, University Park, Pa. 16802.

TABLE 1. SAMPLES AND THEIR LOCATIONS

Catalog No.*	Composition	
1351	Al-77	Mysore District, India
1352	Al-76	Mexican Hat, Utah
1353	Al-68	Mania, Island of Madagascar
1354	Al-67	Fort Wrangle, Alaska
1355	Al-51	Gore Mtn., New York
1356	Py-71	Navajo Indian Reservation, Arizona
1357	Py-59	Macon Co., North Carolina
	Py-Cr (III)	Moravia, Czechoslovakia
1358	Sp-70	Picos de Cavalos, Cerea, Brazil
1359	Sp-53	Gore Mtn., New York
1360	Gr-92	Lake Jaco, Chihuahua, Mexico
1361	Gr-92B	Lake Jaco, Chihuahua, Mexico
1362	Gr-90	Eden Mills, New Hampshire
1363	Gr-89	Trinidad Valley, Baja Calif., Mexico
1364	Gr-87	Trinidad Valley, Baja Calif., Mexico
1365	Gr-74	Baja California, Mexico
1366	An-93	Stanley Butte, Graham Co., Arizona
1367	An-91	Cornwall, Pa.
——	Uv-44	Outokumpu, Finland

* Refers to reference collection of investigators.

TABLE 2. TRACE AND MAJOR ELEMENT ANALYSIS OF SAMPLES, INCLUDING WET CHEMICAL ANALYSIS OF FeO AND Fe_2O_3. ALL RESULTS IN WT. PERCENT

Sample	SiO_2	MgO	MnO	CaO	FeO	Al_2O_3	Fe_2O_3	TiO_2	Cr_2O_3	V_2O_5
Al-77	x	4.70	0.12	1.80	36.00	21.00	0.39	0.01	——	——
Al-76	x	2.20	1.70	6.40	36.73	20.00	0.22	0.06	——	——
Al-68	x	4.25	2.60	1.90	33.58	20.00	0.00	0.05	——	——
Al-67*	40.0	5.45	1.30	2.15	28.80	20.40	x	0.20	0.03	——
Al-51	40.5	8.65	0.52	3.80	23.55	25.00	0.52	0.14	——	——
Py-71*	42.5	20.00	0.39	4.55	8.10	21.80	x	0.16	2.60	——
Py-59*	40.0	15.50	0.82	1.58	17.70	21.20	x	0.33	0.05	——
Sp-70	x	0.20	30.00	——	11.97	25.00	0.27	0.07	——	——
Sp-53*	38.5	0.20	20.90	0.24	18.20	20.00	x	0.02	——	——
Gr-92	x	0.94	0.11	32.00	0.45	23.00	0.45	1.08	——	——
Gr-92B	x	0.67	0.11	32.00	0.44	21.00	0.41	0.52	——	——
Gr-90*	40.0	——	0.26	34.00	x	20.80	4.00	0.06	——	——
Gr-89	x	——	0.16	30.00	1.68	23.00	0.90	0.50	——	0.44
Gr-87	x	——	0.19	27.00	2.08	21.00	0.52	0.64	——	——
Gr-74	x	0.17	1.10	29.00	1.98	20.00	5.03	0.26	——	——
An-94*	39.5	0.30	0.36	31.00	x	1.70	32.00	0.03	——	——
An-93	x	——	0.33	30.00	0.50	1.40	29.83	0.01	0.04	——
Uv-44*	x	1.80	0.62	25.00	x	8.00	6.00	0.23	14.00	0.25
Py-Cr(III)*	x	x	0.30	x	x	x	5.00	x	1.50	x

x = No analysis made.
—— = Concentration below limits of detection.
* = Iron analyses by emission spectrograph only.

size, availability, and phase purity. The localities are listed in Table 1. An attempt was made to obtain samples which would reflect the entire range of crystalline solubility between the end-members. This was accomplished satisfactorily for the pyralstites; however, the middle composition range of the grossularite-andradite series was not obtained.

The samples were characterized by the determination of a using a GE XRD diffractometer and least-squares analysis. Trace and major element analyses were by emission spectrography. Wet chemical analyses for ferrous-ferric ratios were obtained for ten of the samples. Analytical data are given in Table 2.

The approximate molecular proportions of the end-members within each sample were calculated, and the major end-member constituent (abbreviated), and its approximate percentage was used as the sample designation (*i.e.* Al-51 is almandine $\simeq 51\%$). If no ferrous-ferric analyses were made, iron was calculated as FeO in the pyralspites and as Fe_2O_3 in the ugrandites. This information is summarized in Table 3.

The samples were sliced and ground to approximately 0.25 to 0.50 mm thickness. The samples were then polished to a glass finish on three-micron grit.

The absorption data between 0.3 and 2.6 μm were collected on both the Beckman DK-2A and the Cary 14 Spectrophotometers. The spectra run as a function of temperature were obtained using the Cary 14 with a cold cell and liquid nitrogen.

A trio of strong bands in the near infrared is common to most garnet spectra. Pyralspite spectra are quite intense, while ugrandite spectra are rather weak. Manning's assignment of these bands to spin-allowed transitions of Fe^{2+} on the 8-coordinated site appears to be correct. This portion of the spectrum is not shown in our figures and the bands are not discussed further.

Spin-forbidden Transitions of Fe^{3+} and Fe^{2+}

The iron-containing garnets exhibit some of the most complicated visible spectra yet observed in transition ion-containing minerals. These are due mainly to the spin-forbidden transitions of Fe^{3+} and Fe^{2+}.

Ugrandites

The spectra of the ugrandites are less complicated than those of the pyralspites, and the analysis is more straightforward. A typical grossular spectrum is shown in Figure 1, and the frequencies for all ugrandites exam-

TABLE 3. LATTICE PARAMETER AND MOLECULAR PROPORTIONS FOR EACH SAMPLE

Sample	Lattice Parameter (Å)	Py	Al	Sp	Gr	An	Uv
Al-77	11.5019	18.0	77.0	—	4.6	0.4	—
Al-76	11.5127	8.0	76.0	3.6	13.0	—	—
Al-68	11.5292	22.6	67.8	5.0	3.3	1.3	—
Al-67*	11.5167	23.0	67.5	3.0	6.4	—	—
Al-51	11.5160	33.6	51.0	0.9	13.1	1.4	—
Py-71*	11.5302	71.4	16.0	0.9	3.4	1.0	7.3
Py-59*	11.5026	59.1	37.5	1.7	1.7	—	—
Sp-70	11.6116	6.8	22.4	70.0	—	0.8	—
Sp-53*	11.571	0.9	45.5	53.0	0.7	—	—
Gr-92	11.8399	3.1	0.5	—	92.0	4.6	
Gr-92B	11.8412	3.0	0.7	—	92.1	4.4	
Gr-90	11.8478	—	3.2	0.6	89.9	6.4	
Gr-89	11.8486	—	4.3	0.5	89.0	6.4	
Gr-87	11.8412	—	6.0	0.6	87.3	6.4	
Gr-74	11.8512	0.5	4.7	2.6	73.6	18.4	
An-94*	12.033	1.2	—	0.5	4.5	94.0	
An-93	12.0429	—	1.0	0.5	5.5	93.0	

* Assumes all iron is one valence state, Fe^{2+} in pyralspites and Fe^{3+} in ugrandites.

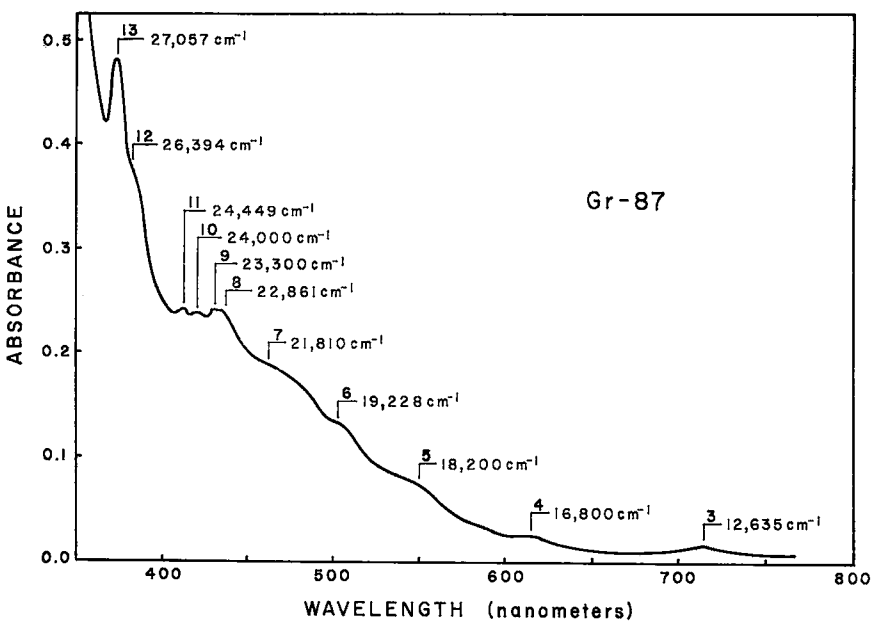

FIG. 1. Absorption spectrum of a typical grossular, Gr-87. Band frequencies are given in cm^{-1}. Each band is labeled by a number.

TABLE 4. SPIN-FORBIDDEN BANDS OBSERVED IN THE UGRANDITES. INTENSITIES AS A/t IN mm^{-1} ARE GIVEN IN PARENTHESES

Sample Band	An-94	An-93	Gr-74	Gr-92B	Gr-89	Gr-92	Gr-87	Gr-90	Assignment
3	—	12453(0.12)	13111(0.04)	12804(0.02)	13108(0.04)	13021(0.02)	12635(0.02)	12600(0.03)	$(Fe^{3+})^{VI}$
4	—	16650(0.07)	—	—	16537(0.02)	17197(0.02)	16800(0.01)	—	$(Fe^{3+})^{VI}$
5	—	—	18000(0.01)	18200(0.01)	—	18433(0.01)	18200(0.01)	—	$(Fe^{3+})^{IV}$
6	—	—	19700(0.02)	20020(0.10)	—	19873(0.01)	19228(0.01)	—	$(Fe^{3+})^{IV}$
7	—	—	21758(0.08)	22100(0.02)	—	22300(0.03)	21810(0.03)	22300(0.12)	$(Fe^{3+})^{IV}$
8	22779(1.60)	22701(1.50)	22865(0.16)	22873(0.06)	22860(0.05)	22832(0.08)	22861(0.05)	22850(0.14)	$(Fe^{3+})^{VI}$
9	22936(0.90)	22999(0.86)	23121(0.18)	23492(0.07)	23700(0.19)	23074(0.08)	23300(0.06)	23120(0.15)	$(Fe^{3+})^{VI}$
10	—	24000(0.09)	23952(0.02)	—	—	—	24000(0.01)	—	$(Fe^{3+})^{VI}$
11	—	24509(0.14)	24480(0.19)	24510(0.02)	—	24444(0.01)	24449(0.03)	24450(0.02)	$(Mn^{2+})^{VIII}$
12	—	—	26400(0.06)	26453(0.04)	—	26428(0.05)	26394(0.04)	26380(0.09)	$(Fe^{3+})^{IV}$
13	—	—	27040(0.29)	27044(0.04)	27042(0.06)	27013(0.05)	27057(0.08)	27000(0.19)	$(Fe^{3+})^{VI}$

ined are listed in Table 4. The spectra of the andradites are similar to those of grossular, except that fewer bands are observed and the spectrum is obscured by the visible shoulder of the charge-transfer bands in the ultraviolet. The reference spectrum of Figure 1 gives a numerical code to each band, and the spectra of all other ugrandites are indexed by this number. Numbers 1 and 2 are the near-infrared bands.

Three criteria can be used for assigning these bands : (i) The intensity of the band should vary linearly with the concentration of the ion to which it is assigned ; (ii) All bands should correspond to some specific energy level of the assigned ion, and (iii) The band frequencies should match those of the energy level diagram with a reasonable choice of crystal field parameters.

Beer's law plots of the various bands in the ugrandite spectra yield reasonable lines as a function of Fe_2O_3 concentration for bands 3, 4, 8, 9, and 13 (Fig. 2). One exception is band 9 in sample Gr-89 which has an intensity independent of the iron concentration. This band appears to be due to vanadium and will be discussed in a latter section. The molar extinction coefficients calculated from the slopes of the Beer's law curves are surprisingly high for spin-forbidden transitions.

Band 8 near 22,000 cm^{-1} and band 13 near 27,000 cm^{-1} have been identified by Manning as the ${}^6A_{1g} \rightarrow {}^4A_{1g}$, ${}^4E_g$ and ${}^6A_{1g} \rightarrow {}^4E_g(D)$ field-independent transitions on the basis of the sharpness of the bands and their agreement with these transitions in other iron-containing compounds. Accepting these assignments, the Racah parameters can be calculated from the relationships

$$\nu(A_{1g}, E_g(G)) = 10B + 5C$$
$$\nu(E_g(D)) = 17B + 5C$$

(see Keester & White 1968, for discussion of the source of these equations). Values of the Racah parameters $B = 614$ cm^{-1} and $C = 3332$ cm^{-1} were used in a computer program (Berkes 1968) to solve the Tanabe-Sugano equations for all Fe^{3+} energy levels. Figure 3 shows the energy level diagram with the positions of the proposed $(Fe^{3+})^{VI}$ bands superimposed. A good match between band frequency and energy level is obtained with a choice of $Dq(\text{oct}) = 1260$ cm^{-1}.

The intensity of band 11 was found to relate to the concentration of Mn^{2+} but not to iron. The correlation was confirmed by comparison with the spectrum of spessartine.

Bands 5, 6, 7 and 12 remain unaccounted for. We have the three possibilities of assigning these to other trace transition ions, to levels split

from the octahedral ones by the distorted crystal field, or to a distribution of Fe^{3+} on sites other than octahedral. Since research on the rare earth garnets has shown Fe^{3+} to occupy the tetrahedral sites we consider the third hypothesis the most likely. The crystal field splitting parameter,

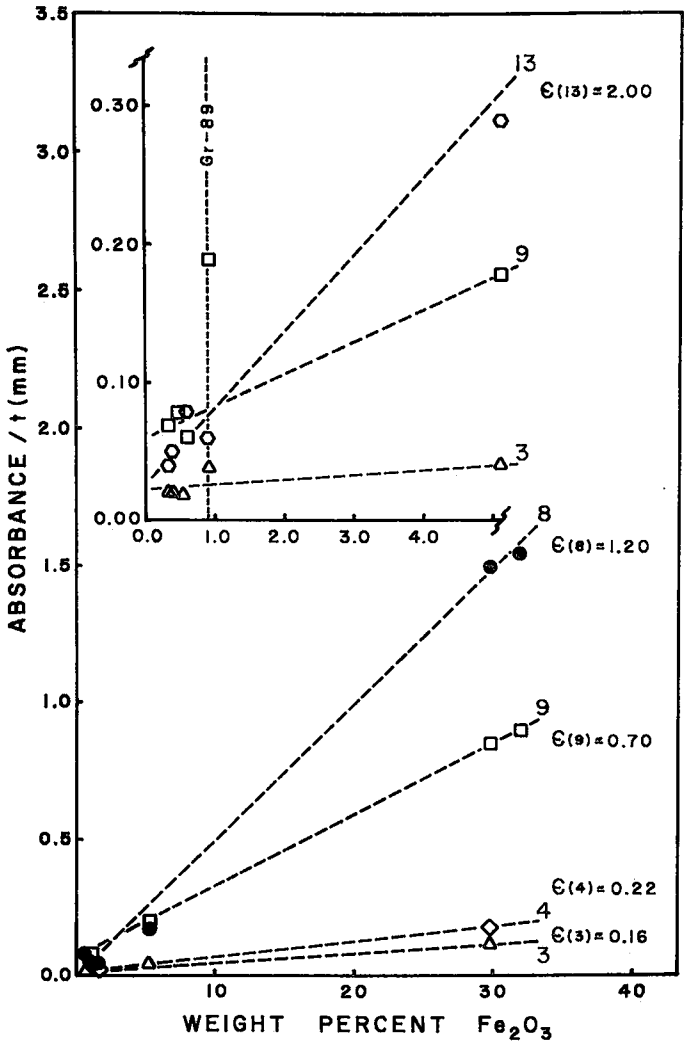

FIG. 2. Beer's law curves for various ugrandite bands. Molar extinction coefficients are given for each numbered band. Exploded view of low-iron region is shown in inset.

Dq, for Fe^{3+} on the tetrahedral sites ought to have a value about 4/9 of the octahedral value or 555 cm^{-1}. The frequencies of bands 5, 6, 7 and 12 are shown on Figure 3 at this *Dq* value and the agreement is seen to be reasonably good. The intensities are low and the concentration of Fe^{3+} on the tetrahedral sites cannot be large. Since the molar extinction coefficient for $(Fe^{3+})^{IV}$ is not known, these intensities cannot be used as a method for determining the site distribution at present. All bands can be accounted for without assuming any splitting due to the S_6 site symmetry

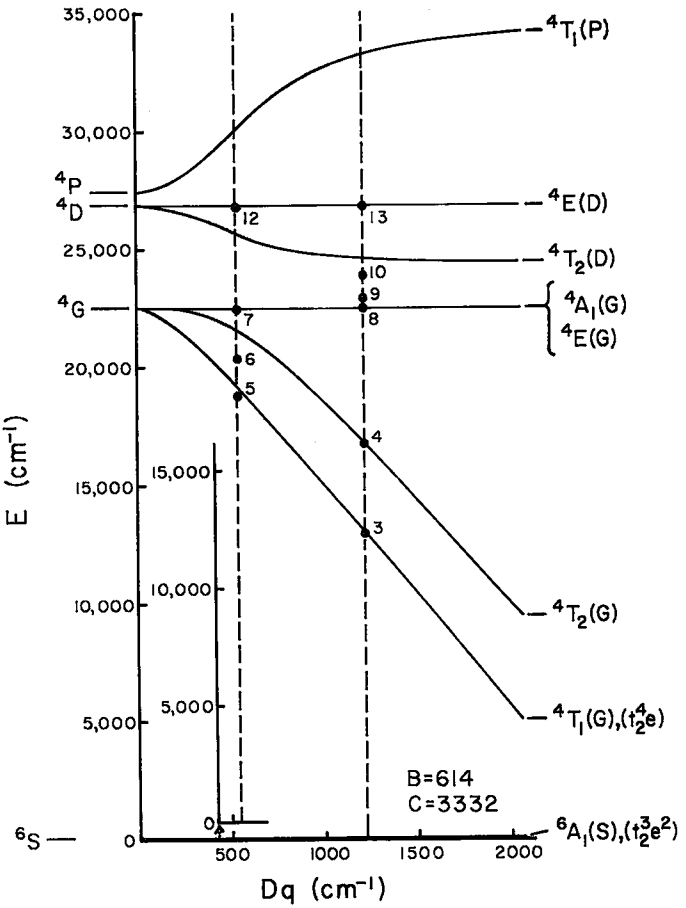

FIG. 3. Energy level diagram for Fe^{3+} in octahedral and tetrahedral coordination.

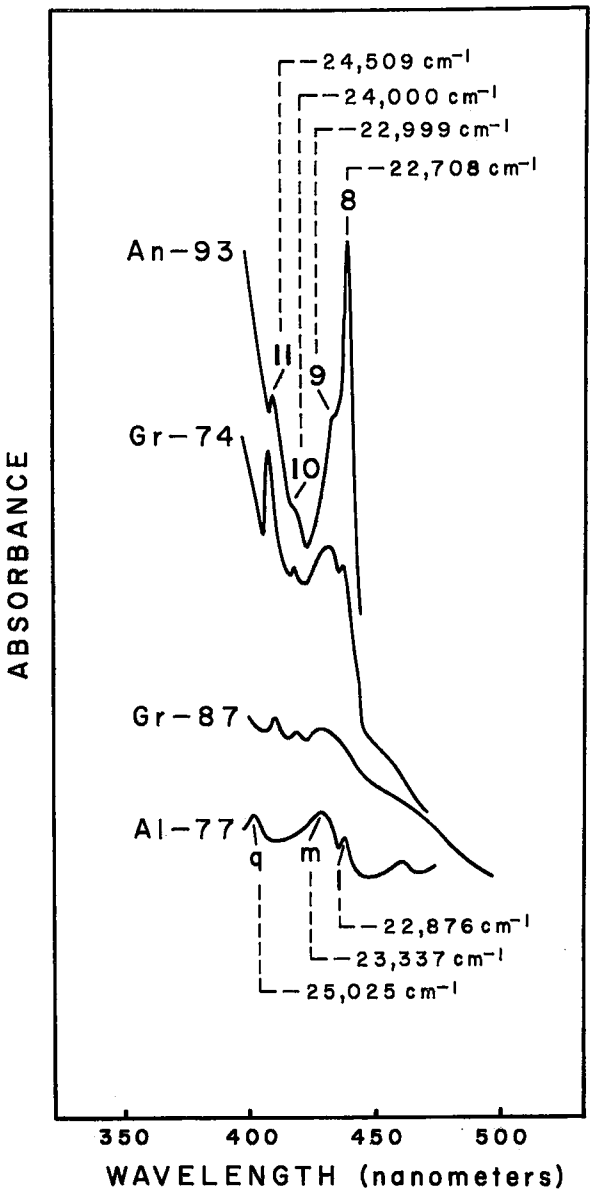

FIG. 4. Varying band shape of ${}^6A_{1g} \rightarrow {}^4A_{1g}$, ${}^4E_g(G)$ transition.

There is one further comment on the shape and the intensity of the first field-independent band of $(Fe^{3+})^{VI}$. The shape of this band changes from the combination of a sharp peak and a weak shoulder in andradite to a doublet of broader weak peaks in grossular (Figure 4). This change in band shape is significant in that the sharp peak found in the andradites was used by Manning to assign the equivalent transition in the pyralspites. It would appear that the assignment would be more or less uncertain at low Fe^{3+} concentrations. The intensity of this band becomes still larger in the titanium garnets (Manning & Townsend 1970).

Pyralspites

The visible spectra of the pyralspites are considerably more complex than the spectra of the ugrandites (Figure 5). The bands are labeled with a lower-case letter. Letters a, b, c refer to the infrared bands not shown in the spectra. Frequencies for all specimens are listed in Table 5. A spectrum of Al-77 taken at liquid nitrogen temperature is also shown in Figure 5. The lower temperature brings out the bands in more detail, but the spectrum is similar in other respects to that measured at room temperature.

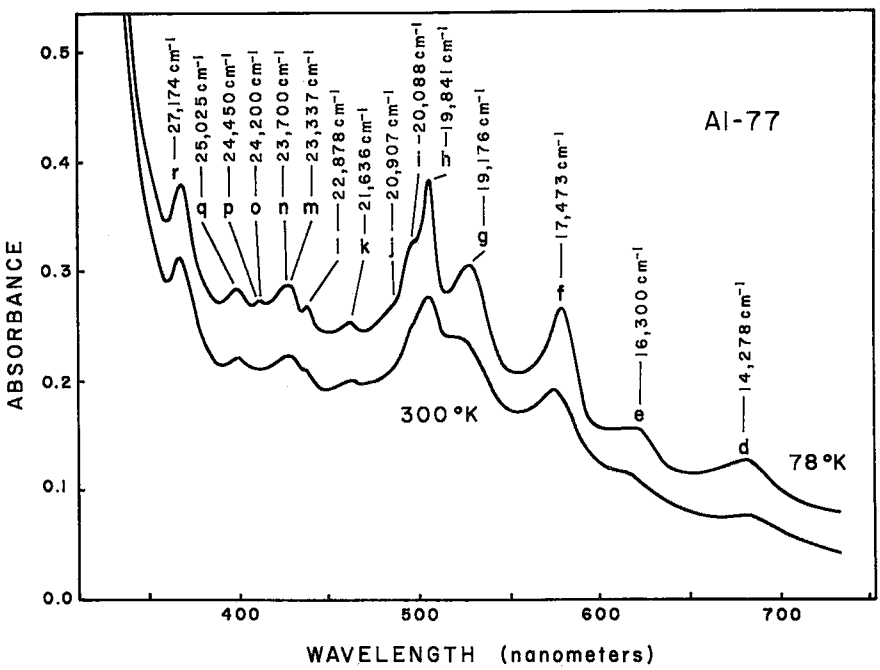

FIG. 5. Absorption spectrum of an almandine at room and liquid nitrogen temperature.

TABLE 5. SPIN-FORBIDDEN BANDS OBSERVED FOR THE PYRALSPITES. INTENSITIES AS A/t IN mm^{-1} ARE GIVEN IN PARENTHESES

Sample Band	Al-77	Al-76	Al-68	Al-67	Al-51	Sp-70	Sp-53	Sp-59	Assignment
d	14278(0.14)	14378(0.15)	14473(0.13)	14327(0.07)	14725(0.10)	14641(0.07)	14619(0.09)	14368(0.06)	$(Fe^{2+})^{VIII}$
e	16300(0.22)	16300(0.24)	16313(0.19)	16155(0.11)	16210(0.15)	16515(0.11)	16667(0.14)	16280(0.07)	$(Fe^{2+})^{VIII}$
f	17473(0.44)	17416(0.47)	17482(0.39)	17483(0.20)	17307(0.29)	17708(0.24)	17575(0.20)	17398(0.12)	$(Fe^{2+})^{VIII}$
g	19176(0.56)	19098(0.53)	19249(0.46)	19231(0.22)	19305(0.36)	19286(0.26)	19157(0.21)	19105(0.15)	$(Fe^{2+})^{VIII}$
h	19841(0.66)	19798(0.62)	19806(0.53)	19802(0.35)	19861(0.46)	19873(0.29)	19802(0.30)	19840(0.21)	$(Fe^{2+})^{VIII}$
i	20088(0.05)	20113(0.06)	20101(0.03)	--	20172(0.01)	20285(0.01)	20100(0.07)	—	$(Fe^{2+})^{VIII}$
j	20907(0.05)	20808(0.05)	20999(0.04)	21242(0.04)	21143(0.03)	20661(0.09)	20600(0.06)	21009(0.03)	Mn^{2+}
k	21636(0.12)	21621(0.09)	21650(0.07)	21692(0.03)	21739(0.04)	21782(0.05)	21671(0.07)	21692(0.05)	$(Fe^{2+})^{VIII}$
l	22878(0.04)	22840(0.04)	—	—	23129(0.16)	—	22936(0.02)	22883(0.01)	$(Fe^{3+})^{VI}$
m	23337(0.16)	23468(0.18)	24557(0.14)	23585(0.11)	23560(0.22)	23321(0.16)	23256(0.17)	23529(0.06)	$(Fe^{3+})^{VI}$
n	—	—	—	—	—	23703(0.46)	23600(0.25)	—	Mn^{2+}
o	—	24242(0.04)	24278(0.02)	24272(0.03)	—	24200(0.25)	24272(0.19)	24200(0.02)	Mn^{2+}
p	—	24533(0.08)	24498(0.13)	24480(0.09)	24367(0.05)	24516(0.88)	24459(0.79)	24450(0.06)	Mn^{2+}
q	25025(0.06)	24931(0.09)	25000(0.05)	—	25000(0.04)	—	—	25063(0.04)	$(Fe^{2+})^{VIII}$
r	27174(0.15)	27114(0.10)	27211(0.07)	27137(0.11)	27226(0.18)	27000(0.12)	27050(0.17)	27248(0.05)	$(Fe^{3+})^{VI}$

Fig. 6 shows Beer's law curves for bands d, e, f, g, and h as a function of ferrous iron concentration. The smooth straight line plots are evidence that these bands should be assigned to Fe^{2+}. Likewise, the molar extinction coefficients calculated range from 0.08 to 0.28, values that are quite reasonable for spin-forbidden transitions. If these bands are assumed to be due to Fe^{3+}, not only do the intensities not follow Beer's law, but the extinction coefficients are in the order of 30 to 40, values that are much too large for spin-forbidden transitions. Bands i, k, and q are weak and difficult to measure, but their intensities as a function of FeO concentration imply that they are also due to Fe^{2+}.

Beer's law plots of bands l, m, and r as a function of ferric iron concentration indicate that they are due to Fe^{3+}. Their frequencies at 22,900, 23,300, and 27,000 are in good agreement with the corresponding bands at 22,800, 23,300, and 27,000 cm^{-1} in the ugrandites. In addition, the calculated molar extinction coefficients are in the range of 1.5 to 3.0, also in good agreement with the values found for the ugrandites.

Eleven of the fifteen bands found in the pyralspites can be assigned to iron. It will be shown that the remaining four bands, j, n, o, and p, arise from Mn^{2+}.

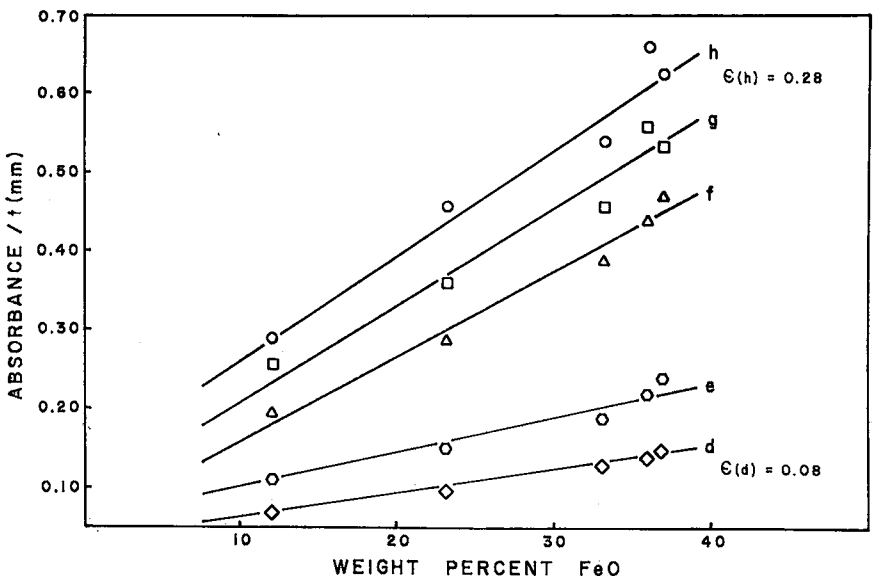

Fig. 6. Beer's law plot of d-h bands of pyralspites. ε-values are the molar extinction coefficients.

Specific crystal field assignments for the spin-forbidden transitions of Fe^{2+} on the garnet cubic site are difficult because of the large number of energy levels clustered close together and because of the unknown effect of the orthorhombic crystal field. A further difficulty arises because there is no convenient way to estimate the Racah parameters and thus to construct a Tanabe-Sugano diagram specific to the garnet site. A computer-drawn diagram utilizing best-fit values of $B = 890$ and $C = 4000$ cm^{-1} is shown in Figure 7. The values of Dq was fixed at 600 cm^{-1} from the spin-allowed bands, and this is indicated by the vertical line on the diagram. The observed spin-forbidden bands are shown as solid circles on this line.

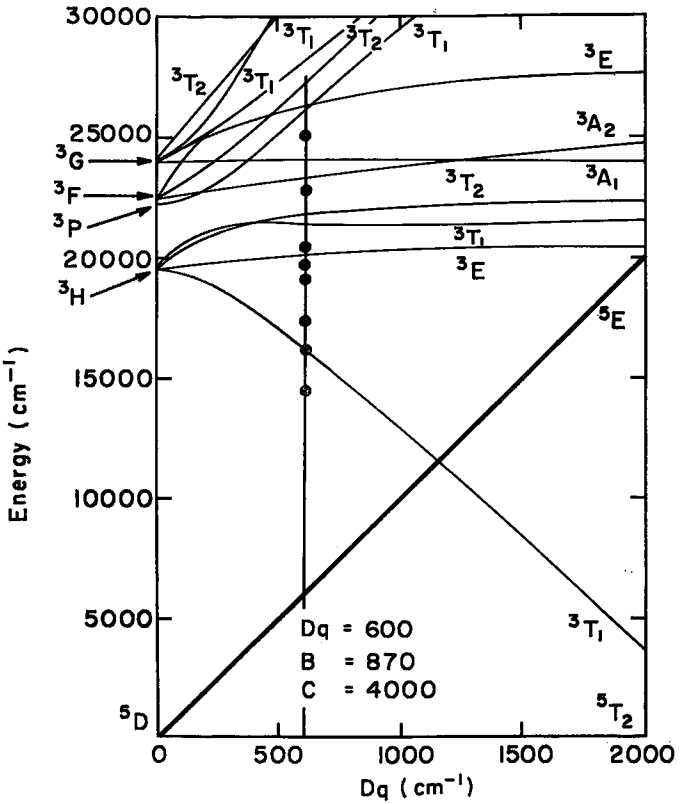

FIG. 7. Tanabe-Sugano energy level diagram for Fe^{2+}. Diagram assumes cubic crystal field and does not take into account the additional band splitting due to D_2 symmetry. Frequencies of Fe^{2+} bands are indicated by black circles. Singlet levels are not shown.

Three bands are expected from the D_2 splitting of ${}^3T_{1g}(H)$ level with D_2 group designations ${}^3B_1$, ${}^3B_2$ and ${}^3B_3$. These three levels would be expected to split by a centre of gravity rule since interaction with other levels is not likely. The three experimentally observed bands, d, e, and f, with frequencies of approximately 14,500, 16,300, and 17,400 cm^{-1} may be these levels. These levels increase in frequency as a and temperature increase (Dq decreases) by about 500 cm^{-1}. This would be expected if these bands were derived from the steeply sloping ${}^3T_{1g}(H)$ level.

Bands g and h at 19,200 cm^{-1} and 19,800 cm^{-1} occur as a doublet with the h band being relatively sharp. These two bands vary in frequency between samples by a maximum of 207 cm^{-1} for band g and 75 cm^{-1} for band h, considerably less than the other three bands. Similarly, as temperature increases (Dq decreases) the frequency of these bands remains essentially constant. Thus these bands behave as field-independent transitions. The energy level diagram indicates that the ${}^3E_g(H)$ level is nearly field independent. This level will split into a ${}^3A$ and a ${}^3B_1$ level with expected transition energies of about 20,000 cm^{-1}.

The i band at approximately 20,100 cm^{-1} varies in frequency by 200 cm^{-1} and is a very weak shoulder on the h band. From the energy level diagram, six transitions would be expected from the splitting of the ${}^3T_{1g}(H)$ and ${}^3T_{2g}(H)$ levels. However, these levels are nearly degenerate, and the large number of D_2 levels arising from them would be expected to interact and in many cases would be accidentally degenerate. In addition, there are a number of bands in this region of the spectra (20,000 to 24,500 cm^{-1}) that are due to other ions. Thus the only bands that can reliably be assigned to the splitting of these levels are the i band and probably the k band at approximately 22,800 cm^{-1}. A final band occurring at approximately 25,000 cm^{-1} (q) would be expected to arise from the nearly degenerate ${}^3A$ (F and G) levels.

Manning (1967b) did not reach definite assignments for the complicated visible bands of the pyralspites. By using the Beer's law dependence to sort out the ions, and the computer-generated energy level diagrams to check the consistency of individual assignments, all bands can be fitted. The lower frequency portion of the spectrum is dominated by the spin-forbidden bands of ferrous iron, split by the highly distorted orthorhombic field of the 8-fold site.

Spectra of other Transition-metal Ions in Garnet

Certain spectral features in the silicate garnets can be best assigned to traces of Mn^{2+}, V^{3+}, or Cr^{3+}. In this section these bands are compared

with the spectra of manganese and chromium garnets and various crystal field parameters are calculated.

Manganese garnets

The j, n, o, and p bands of the pyralspites (Table 5) and band 11 of the ugrandites (Table 4) appear to correlate with the manganese rather than the iron concentration. These may be compared with the spectrum of a spessartine in Figure 8. Beer's law plots in Figure 9 show the variation in intensity of these bands with concentration of MnO. Calculated molar extinction coefficients are noted on Figure 9 and are of the expected order of magnitude for spin-forbidden bands.

Manning (1967b) observed the spectrum of a spessartine and found that an intense sharp doublet occurred at approximately 24,500 cm^{-1}, and two very broad and probably composite bands occurred at 23,500 and 21,000 cm^{-1}. In addition, he observed a number of weaker bands which he assigned to iron in one or more of its valence states.

The bands assigned to Mn^{2+} by Manning are equivalent to our j, n, o, and p bands. The o and p bands at approximately 24,000 and 24,500

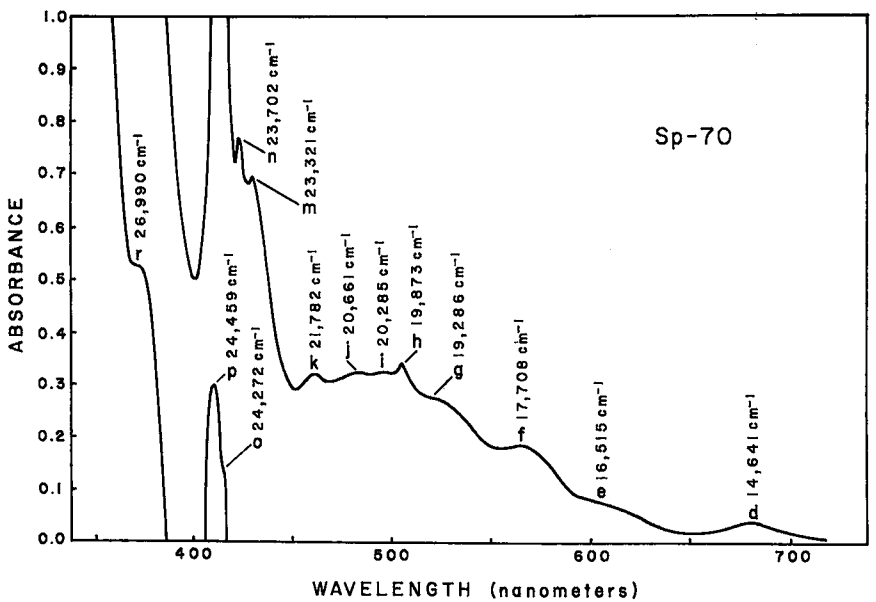

FIG. 8. Visible region of the spectrum of a spessartine, Sp-70. The labeling of the bands is that used for the pyralspites.

cm^{-1} respectively form a doublet in which the p band is very intense and sharp, with the o band forming a weak shoulder on the low-frequency side. Ugrandite band 11 at approximately 24,500 cm^{-1} would appear to be equivalent to the p band in the pyralspite. Manning assigns the band at approxiately 20,800 cm^{-1} (j) to the ${}^6A_{1g} \rightarrow {}^4T_{1g}$ transition, the band at approximately 23,500 cm^{-1} (n) to the ${}^6A_{1g} \rightarrow {}^4T_{2g}$ transition and the doublet at approximately 24,500 cm^{-1} (o and p) to the ${}^6A_{1g} \rightarrow {}^4A_{1g}$, ${}^4E_g$ field independent transition.

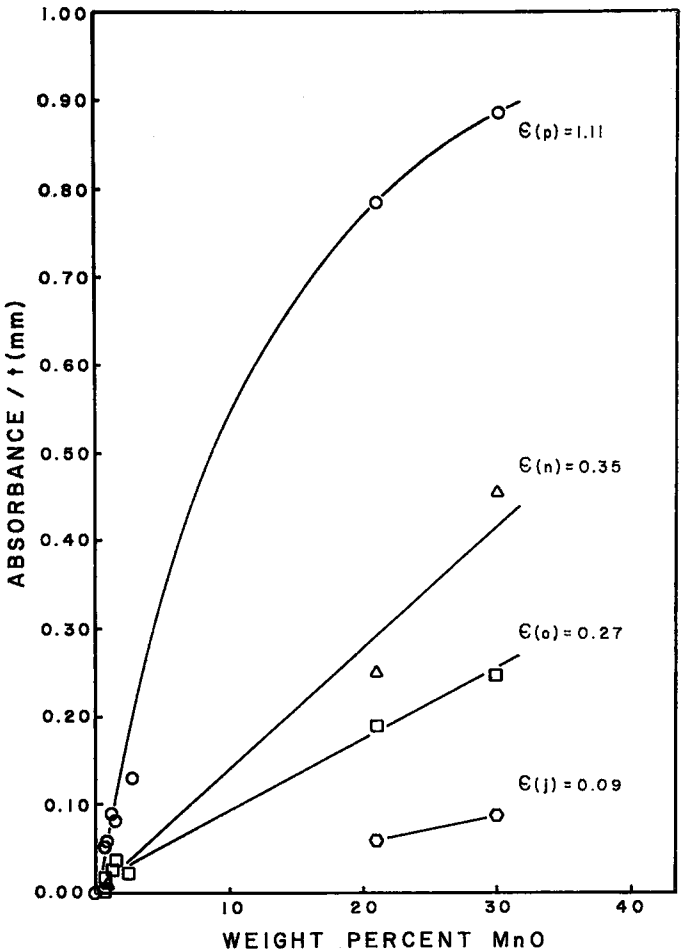

FIG. 9. Beer's law plot for bands assigned to Mn^{2+}.

Since the second field-independent transition was not observed, the Racah parameters cannot be calculated directly. Using typical values for other manganese minerals (Keester & White 1968), good agreement with Manning's assignments was obtained between the energy level diagram and the observed bands with a choice of $B = 664$ cm^{-1}, $C = 3560$ cm^{-1}, and $Dq = 700$ cm^{-1} (Figure 10). Dq for Mn^{2+} in the garnets is lower by about 100 cm^{-1} than Dq for Mn^{2+} on octahedral sites in various other minerals. The lowering of Dq due to the 8-fold coordination of the Mn^{2+} site in garnet is of the order of magnitude expected from crystal field theory (Dq (cube) $= -8/9$ Dq (oct)). Additional splittings of the Mn^{2+} bands due to the D_2 site symmetry were not observed.

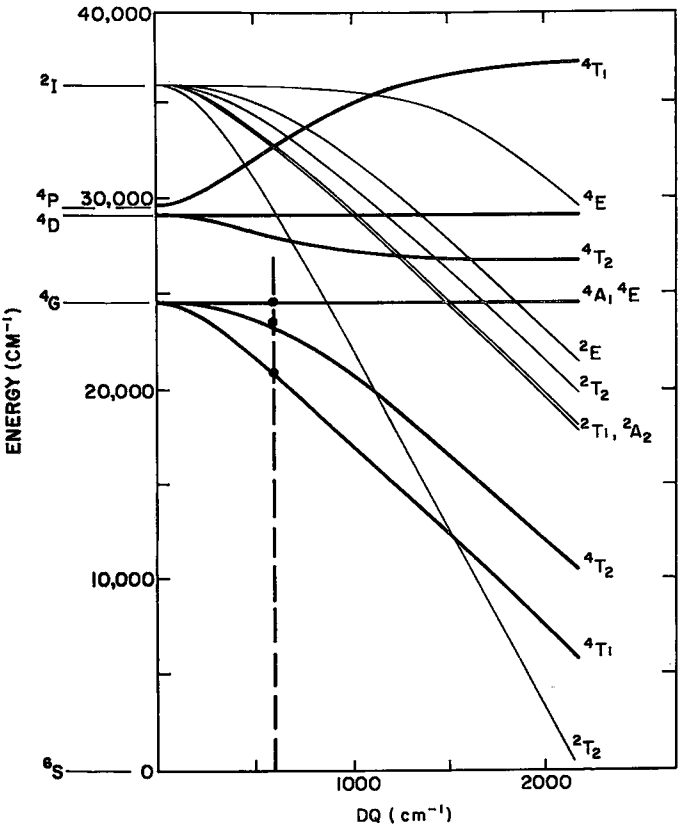

FIG. 10. Energy level diagram for Mn^{2+} (d^5) with $B = 664$ and $C = 3560$cm^{-1}. Vertical line with solid circles shows position of observed Mn^{2+} bands.

Vanadium-containing garnets

One grossular, Gr-89, contains 0.44 wt percent V_2O_5. The spectrum of this garnet contains bands with enhanced intensity at 13,108 and 23,700 cm^{-1}. These appear to be due to V^{3+} on the octahedral sites.

V^{3+} with a d^2 electron configuration has a ${}^3T_{1g}(F)$ ground state in an octahedral field. Unlike most transition ions, the excited triplet levels cross at low field values and the sequence of excited states is : ${}^3T_{2g}(F)$, ${}^3T_{1g}(P)$, and ${}^3A_{2g}(F)$. The two bands observed would correspond to the ${}^3T_{2g}(F)$ and ${}^3T_{1g}(P)$ levels. The third spin-allowed band lies at quite high energies and is not usually observed. A comparison may be made with the spectrum of V^{3+} in corundum (McClure 1962, White *et al.* 1967) where the two levels are found at 17,500 and 25,300 cm^{-1}. In the absence of the third band, Dq and B cannot be conveniently calculated. However, Dq will be on the order of 1630 cm^{-1} in garnet, lower than the 2175 cm^{-1} found for corundum.

Chromium-containing garnets

Three specimens, Py-71, Py-Cr(III), and Uv-44, contain significant quantities of Cr^{3+} and their spectra (Figure 11) contain broad intense bands characteristic of spin-allowed transitions. Their spectra are representative of Cr^{3+} in octahedral coordination. The agreement in measured band frequency with data by Manning (1967b) and Poole (1964) for chromium-pyrope and with Manning (1969) for uvarovite is excellent.

Band frequencies and assignments are listed in Table 6. These two bands can be used to calculate both Dq and B using the relations

$$Dq = \frac{1}{10}\nu_1$$

$$B = \frac{1}{3}\frac{(2\nu_1 - \nu_2)(\nu_2 - \nu_1)}{(9\nu_1 - 5\nu_2)}$$

obtained by solving the Tanabe-Sugano matrices analytically. These parameters are also listed in Table 6. No additional splitting due to the S_6 site symmetry was obsered.

The colour of uvarovite is green, while that of the pyropes is blood red. This colour change arises because of a shift in the visible window between the two main bands that occurs because of the shift in band frequencies. The shift is due to the increase in Dq that occurs when the smaller aluminum site in pyrope is expanded to the large chromium site in uvarovite. The colour change is similar to that observed between ruby and chromium oxide. However, Racah B remains constant in the garnet

series, whereas a shift in B as well as a shift in Dq are observed in the ruby-Cr_2O_3 series.

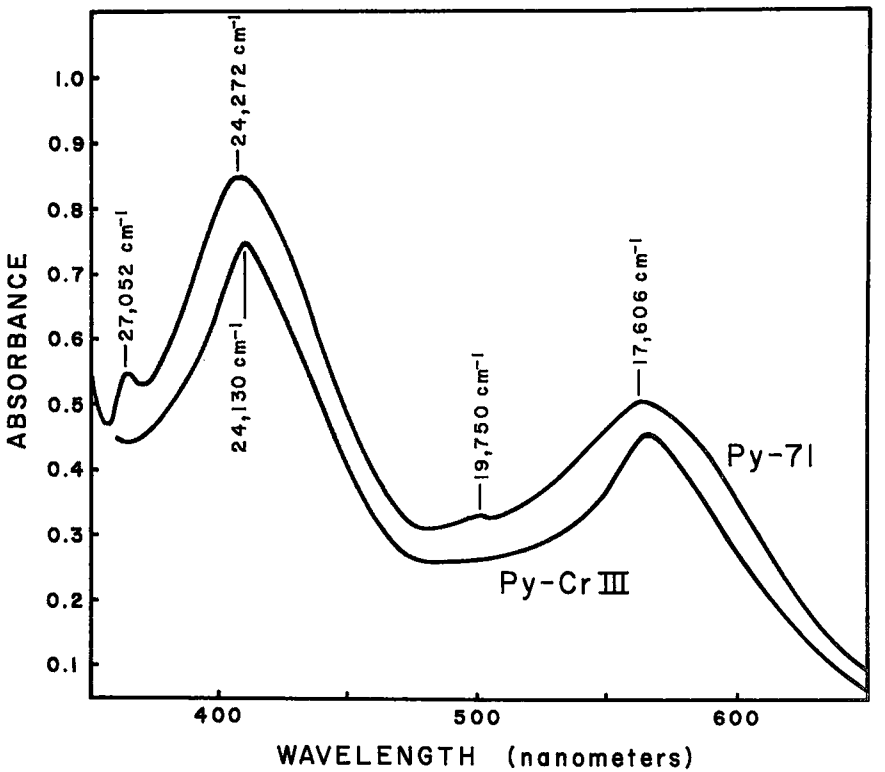

FIG. 11. Spectra of high-chromium pyropes.

TABLE 6. CRYSTAL FIELD DATA FOR CHROMIUM GARNETS

	Py-71	Py-Cr(III)	Uv-44
$\nu_1(cm^{-1})$	17,606	17,606	16,191
$\nu_2(cm^{-1})$	24,272	24,130	22,676
$\varepsilon(\nu_1)$ (liter mole^{-1}cm^{-1})	12	12	—*
$\varepsilon(\nu_2)$ (liter mole^{-1}cm^{-1})	21	20	—
$Dq(cm^{-1})$	1,761	1,761	1,617
$B(cm^{-1})$	660	655	653

* Spectra obtained by diffuse reflectance from powders. Accurate intensities not measurable.

Conclusions

The visible spectra of natural silicate garnets are among the most complex observed in minerals. Contributions to spectral bands arise from the ions Fe^{2+}, Fe^{3+}, Mn^{2+}, Cr^{3+} and V^{3+}. The site distribution of these ions, however, is apparently fixed by crystal chemical considerations. Fe^{2+} and Mn^{2+} appear to mainly on the cubic site, whereas Fe^{3+}, Cr^{3+}, and V^{3+} occur mainly on the octahedral site. The D_2 site symmetry of the cubic site splits the degenerate energy levels of the ions that occur there and introduces additional complexity in the spectra. Although the octahedral site has S_6 symmetry, the distortion is small and no evidence for splitting of the octahedral levels was found in the spectra.

An exception is the distribution of Fe^{3+} which populates both octahedral and tetrahedral sites in the ugrandite garnets. Tetrahedral ferric iron occurs in high concentrations in the rare earth iron garnets. A detailed comparison of the bands due to iron on the two sites and the derived crystal field parameters is given in Table 7. Because the distribution of Fe^{3+} between the 6-fold and 4-fold sites is likely to vary depending on the genesis of the particular garnet, the optical spectrum may provide a useful tool for the determination of site distribution.

Table 7. Summary of Fe^{3+} Spectra in Natural Silicate Garnets and in Yttrium Iron Garnet

Tetrahedral Site		Octahedral Site		
YIG *	Silicate Garnet	YIG *	Silicate Garnet	
16,400 cm^{-1}	18,400 cm^{-1}	11,000 cm^{-1}	13,000 cm^{-1}	${}^6A_{1g} \rightarrow {}^4T_{1g}(G)$
20,400	20,000	14,280	17,000	$\rightarrow {}^4T_{2g}(G)$
21,000	22,000	20,400	22,700	$\rightarrow {}^4A_{1g}, {}^4E_g(G)$
26,300	—	23,000	24,000	$\rightarrow {}^4T_{2g}(D)$
		23,870		
26,670	26,400		27,000	$\rightarrow {}^4E_g(D)$
		24,700		
620	580	1,200	1,280	$Dq(cm^{-1})$
900	600	700	600	$B(cm^{-1})$
2,400	3,100	2,600	3,300	$C(cm^{-1})$

* Data from Wood & Remeika (1967).

Acknowledgement

This work was supported by the National Science Foundation under Grant GP 3232. We are indebted to Dr. J. S. Berkes for use of his Tanabe-Sugano Computer program and to Dr. P. G. Manning for the contribution of a uvarovite specimen and for a useful discussion of the assignments.

References

Berkes, J.S. (1968) : Energy level diagrams for transition metal ions in cubic crystal fields. *MRL Monog.* **2,** Materials Research Laboratory, The Pennsylvania State University.

Keester, K.L. & White, W.B. (1968) : Optical absorption spectra and chemical bonding in manganese minerals. *Proc. Vth Internat. Mineral. Assoc. Meet., Min. Soc. London*, 22.

Manning, P.G. (1967a) : The optical absorption spectra of some andradites and the identification of the $^6A_1 \rightarrow {}^4A_1{}^4E(G)$ transition in octahedrally bonded Fe^{3+}. *Canad. Jour. Earth Sci.* **4,** 1039.

———— (1967b) : The optical absorption spectra of the garnets almandine-pyrope and spessartine and some structural interpretations of mineralogical significance. *Canad. Mineral.* **9,** 237.

———— (1969) : Optical studies of grossular, andradite (var. colophonite) and uvarovite. *Canad. Mineral.* **9,** 723.

———— (1970a) : Racah parameters and their relationship to lengths and covalencies of Mn^{2+} -and Fe^{3+} -oxygen bonds in silicates. *Canad. Mineral.* **10,** 677.

———— (1970b) : Compositions of garnets in interstellar dust. *Nature* **227,** 1121.

———— & Townsend, M.G. (1970) : Effect of next-nearest neighbor interaction on oscillator strengths in garnets. *J. Phys. C: Solid State Phys.* **3,** L14.

McClure, D.S. (1962) : Optical spectra of transition metal ions in corundum. *J. Chem. Phys.* **36,** 2757.

Poole, C.P. (1964) : Theoretical spectra and color of chromium-containing solids, *J. Phys. Chem. Solids* **25,** 1169.

White, W.B., Roy, R. & Chrichton, J. McK. (1967) : The "alexandrite effect" : an optical study. *Amer. Mineral.* **52,** 867.

Wood, D.L. & Remeika, J.P. (1967) : Effect of impurities on the optical properties of yttrium iron garnet. *J. Appl. Phys.* **38,** 1038.

Manuscript received August 1971, emended October 1971.